The Journal of the Korean Society of
Coastal and Ocean Engineers
Vol. 7, No. 1, pp. 75~90, March 1995

The Effect of Internal Flow on Marine Riser Dynamics
Riser의 內部流體 흐름이 Riser 動的反應에 미치는 影響

Nam Seeg Hong*
洪 南 植

Abstract □ A mathematical model for the dynamic analysis of a riser system with the inclusion of internal flow and nonlinear effects due to large structural displacements is developed to investigate the effect of internal flow on marine riser dynamics. The riser system accounts for the nonlinear boundary conditions and includes a steady flow inside the pipe which is modeled as an extensible or inextensible, tubular beam subject to nonlinear three dimensional hydrodynamic loads such as current or wave excitation. Galerkin's finite element approximation and time incremental operator are implemented to derive the matrix equation of equilibrium for the finite element system and the extensibility or inextensibility condition is used to reduce degree of freedom of the system and the required computational time in the case of a nonlinear model. The algorithm is implemented to develop computer programs used in several numerical applications. The investigations of the effect of internal flow on riser vibration due to current or wave loading are performed according to the change of various parameters such as top tension, internal flow velocity, current velocity, wave period, and so on. It is found that the effect of internal flow can be controlled by the increase of top tension. However, careful consideration has to be given in the design point, particularly for the long riser under the harmonic loading such as waves. And it is also found that the consideration of nonlinear effects due to large structural displacements increases the effect of internal flow on riser dynamics.

要 旨 : 본 硏究에서는 riser 內部의 流體흐름에 의해 發生하는 流體力이 深海低 riser의 動特性에 미치는 影響에 관해 調査하였다. riser의 非線形 動的解析을 위해 riser 內部의 流體흐름을 시스템에 包含하여 數學的 모델을 誘導하였으며 誘導된 모델에 Galerkin의 有限要素近似法과 時間增分子를 適用함으로써 數値解析을 위한 모델을 開發하였다. 또한 시스템의 自由度를 줄이고 非線形모델의 數値解를 얻기위해 행해지는 反復計算을 줄이며 正確度를 높이기 위해 riser의 軸方向 extensibility 條件을 使用하였다. 管內部 流體 흐름으로 인한 riser의 動特性에 미치는 影響을 上部 引張力, 潮流速度, 波週期 등과 같은 여러 影響要因들을 變化시키면서 調査하였다. 數値解析 결과 內部流體 흐름으로 인한 影響을 줄이기 위해서는 riser의 上部에 引張力을 riser의 許容內力 限度내에서 增加시키는 方法이 있으나 深海低로 갈수록 引張力 增加에 限界가 있기 때문에 riser 周圍에 浮體를 附着시키는 方法이 提示된다. 이 이외에도 riser의 解析시 大變形으로 인한 非線形性을 考慮하게 되면 內部 流體흐름이 riser의 動特性에 미치는 影響을 增加시킴을 알 수 있었다.

1. INTRODUCTION

The offshore industry is moving into deeper waters and more hostile environments. When exploratory drilling operations move into deeper water, the dynamic behaviors of riser should be more carefully considered because of the long free span. There are many factors that influence on the behavior of a riser, such as the offshore environment (wave and current), the behaviors of platform (movements or mean offsets), and the properties of the riser itself (dimensions, weight, top tension, and internal flow). Most of these factors have been considered in earlier studies and many related papers have been pu-

*三星建設株式會社 技術硏究所 (Institute of Technology, Samsung Engineering & Constrution Co., Ltd., Kangnam P.O. Box 1430, Seoul, Korea 135-080)

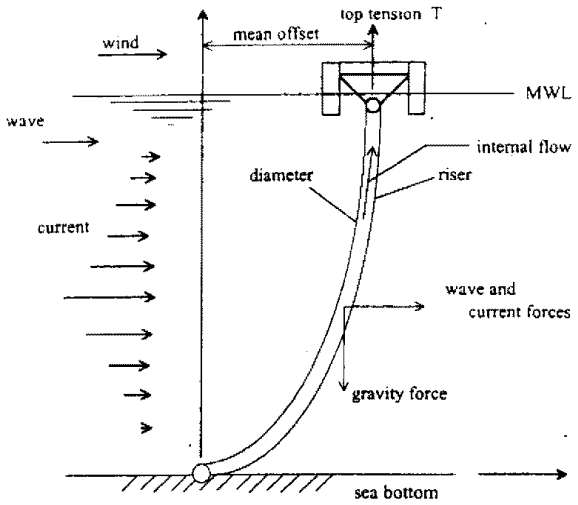

Fig. 1. Configuration of riser system with the inclusion of internal flow.

blished. However, it was not until the publication of a paper (Moe and Chucheepsakul, 1988) that the effect of internal flow on riser dynamics was investigated. Before Moe's investigation it was already known that the internal flow might cause a dynamic instability or buckling of a horizontal pipeline supported above ground and such effect has been considered in the design and analysis of pipeline. Although the dynamics of pipe conveying fluid has been studied fairly extensively over the past 40 years, the basic techniques were recently adopted for the dynamic analysis of a marine riser with internally flowing fluid.

Figure 1 is a schematic diagram of a marine riser conductor that contains internal fluid flow and is subject to environmental forces. When the internal fluid travels inside the curved path along the deflected riser, it experiences centrifugal and coriolis accelerations due, respectively, to the curvature of the riser and the relative motion of fluid to time dependent riser motion. Those accelerations exert against the riser which, in turn, affect the dynamic behavior of the riser and cause riser vibrations. In addition to this interaction problem, the riser behavior is also nonlinear. The nonlinearities are mainly of two origins that result from flow-induced drag force and from geometric nonlinearities due to large structural deflections. The later becomes particularly significant for long risers. Such nonlinearities are due to large deflections and slopes, three-dimensional bending, extensibility, torsion, dependency of the hydrodynamic loads on the riser deformation and nonlinear boundary conditions.

The hydrodynamic loading exerted on the riser depends on the orientation of the riser tubes with respect to the surrounding flow and is deformation dependent. The displacements resulting from these nonlinear effects, in turn, modify the particle motion of the internal fluid. The system becomes a complicated interaction proboem. In summary, the primary objectives of this study are 1) to develop a mathematical model for the analysis of the riser system with the inclusion of internal flow and the aforementioned nonlinear effects, 2) to solve the model numerically, and 3) to examine the effect of the internal flow on riser dynamics. In this study, Galerkin's finite element approximation process is implemented. The effect of internal flow on wave-induced vibration, internal stresses as well as the kinematics of riser are investigated according to the change of internal flow or current velocity, water depth, top tension, wave period and so on. There are only a few papers dealing with the effect of internal flow on marine riser dynamics. Moe (1988) was the first who considered the forces due to the internally flowing fluid as a dynamically forcing component acting on the interior wall of the riser and derived the governing equation of motion. Before that, the loading due to the internal fluid was included in the internal tension of the riser as a fluid static force, that is, centrifugal and Coriolis acceleration due to the internal flow were largely negligible. Wu and Lou (1991) developed a mathematical model for the lateral bending vibration of a marine riser and examined the effect of internal flow and bending rigidity of the pipe on the dynamic behavior of the riser. Their mathematical model included the steady flow inside the pipe together with other factors such as currents or wave excitation and used a singular perturbation technique to solve it under the condition that the rigidity parameter, $\varepsilon = EI/L^3$, is sufficiently small for deep water risers. It was found from their results that the internal flow reduced the effect of top tension, but the riser motion was not significantly affected when the top tension of the riser was relatively high. However, the prob-

lem deserves further investigation since the system solved was linear and the perturbation technique was not valid for low top tension cases. Chen (1992) derived the governing equation with the inclusion of dynamic force for lateral vibration by applying Hamilton's principle. The natural frequencies and the mode shapes were formulated and presented. The critical buckling and significant velocities which associate the internal flowing fluid with system integrity were also presented. In his paper, it was concluded that the natural frequencies could be reduced drastically by the fluid dynamic force if the tension was insufficient for a neutrally buoyant riser system, and that the dynamic force had less influence on a positively or negatively buoyant riser system. However, his system is also a linear model as was that of Wu and the method employed by him to estimate the natural frequencies and the modal shapes appeared to be quite approximate.

For the riser analysis without considering the effect of internal flow, considerable efforts have been made over the years. For linear analysis, several methods, e.g., finite difference, finite element method, or analytical method, etc., were used Burke (1974) studied the dynamic riser response and discussed the effects of increasing water depth on riser design and operations. Dareing and Huang (1979) explored the application of modal analysis for calculating marine riser time-dependent stresses. Chakrabati and Frampton (1982) presented a review on riser analysis techniques.

With increasing water depth, the nonlinear behaviors of the riser become more prominent as mentioned above. The equations for large amplitude three-dimensional inextensional motions of beams were derived by Nordgren (1974), with the assumption of constant principal moments of inertia, negligible rotatory inertia, and the uncoupled torsional motion. Bruce and Michael (1977) described a mathematical model and solution technique for a system with coupled dynamic axial and lateral responses of a riser column. Fellipa and Chung (1981) implemented a finite element method for solving nonlinear static equilibrium configurations of deep water risers. Also, a transient analysis was developed by Chung (1981) for the determination of nonlinear motion by considering nonlinear static configuration as an initial condition for dynamic analysis. Garrett (1982) presented a three-dimensional finite element model of an inextensible elastic rod with equal principal stiffness. The model permitted large deflections and finite rotations and accounted for tension variation along its length. Konuk (1982) provided a general foundation for developing rigorous formulation of problems involving marine pipelines with twist. Safai (1983) developed a method for automatically updating the structural geometry during the dynamic analysis for a system in which the bending, axial and torsional vibrations are uncoupled. Kim and Triantafyllou (1984) studied the nonlinear dynamics of long, slender cylinders assuming moderately large deformations and no longitudinal excitation modes. McNamara and Lane (1984) presented an efficient method based on the finite element approach using convected coordinates for arbitrary large rotations. Huang and Chucheepsakul (1985) introduced a method of static analysis for risers experiencing large displacements. The method represented a modified functional involving multipliers to account for the are length being unvaried with neglected tension, and used the exact curvature of radius in their formulation. Kokarakis and Bernitsas (1985) formulated the problem of static three-dimensional nonlinear, large deformation response of a riser within small strain theory and then solved it numerically by using an incremental finite element algorithm, which involved a prediction-correction scheme. Later, they (Bernitsas and Kokarakis, 1987) employed a previously formulated static model for the dynamic analysis of riser and developed an efficient algorithm for its numerical solution. O' Brien and McNamara (1988) developed a technique based on finite element method by the separation of the rigid body motions from deformations of element under the condition of finite rotations.

2. GOVERNING EQUATION

2.1 Equations of the Pipe

The main aspects of the curved geometry of the system are depicted in Figure 2. Three coordinates systems are defined, namely

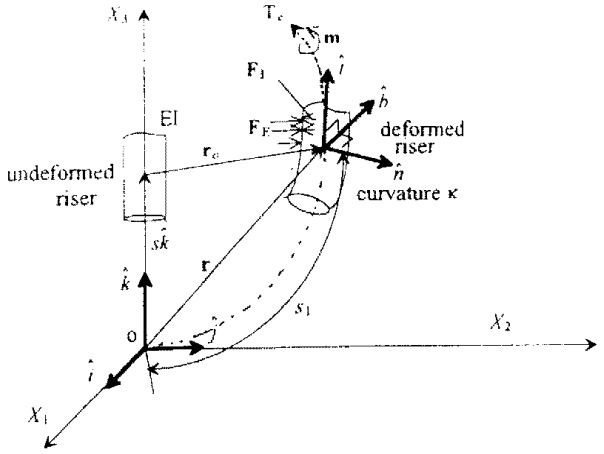

Fig. 2. Position vector and principal direction at a point on the riser centerline.

· $(\hat{I}, \hat{J}, \hat{K})$, an orthonormal global inertial system of coordinates with origin at the lower ball joint of the riser.

· $(\hat{n}, \hat{b}, \hat{t})$, an orthonormal triad passing through the centroid of the cross section of the deformed configuration.

· $(\hat{N}, \hat{B}, \hat{T})$, an nonorthonormal triad passing through the centroid of the cross section of the deformed configuration.

where "^" indicates a unit vector and hereafter boldface represents general vectors. Since we assume no shear deformation, the third nonorthonormal triad becomes consistent with the second orthonormal triad. The initial undeformed configuration of the riser is vertically straight, i.e., its direction accords with $\hat{k}$. The deformed space curve is specified by giving its position vector $\mathbf{r}$ from the origin of space fixed system $(\hat{i}, \hat{j}, \hat{k})$ to a point on the deformed riser centerline (see Fig. 2), as a function of deformed are length s_1. At any point on the deformed curve the unit tangent vector $\hat{t}$, the unit normal vector $\hat{n}$, and the unit binomial vector $\hat{b}$ are defined by

$$\hat{t}=\mathbf{r}', \quad \hat{n}=\hat{t}'/\kappa, \quad \hat{b}=\hat{t}\times\hat{n} \tag{1}$$

where prime denotes differentiation with respect to s_1, and the curvature κ, from the well known results about the differential geometry of curves in space (Love, A., 1927), is given by

$$\kappa^2=\mathbf{r}''\cdot\mathbf{r}'' \quad \text{or} \quad -\mathbf{r}'\cdot\mathbf{r}''' \tag{2}$$

where " · " denotes inner product of vectors (dot product).

The total bending moment, as shown in Fig. 2, acts in the binomial direction and is proportional to the bending rigidity of the cross section EI, and the space curve will be identified with the central axis of the riser in the deformed state, with the position vector, as shown in Fig. 2, represented as follows.

$$\mathbf{r}=\mathbf{r}_0+s\hat{k}=x_1\hat{i}+x_2\hat{j}+(s+x_3)\hat{k} \tag{3}$$

where $\mathbf{r}_0$ is the deformation vector at any point on the riser in the undeformed state.

In the classical theory of rods, the internal state of stress at a point on the rod is fully characterized by the resultant force $\mathbf{F}$ and the couple moment $\mathbf{M}$ acting on the central axis. Conservation of linear momentum and angular momentum leads to the following vector equation of motion.

$$\begin{aligned}&-(EI\mathbf{r}'')''+[(T_c-EI\kappa^2)\mathbf{r}']'+(\mathbf{r}'\times\mathbf{m})'+(H\mathbf{r}'\times\mathbf{r}'')'\\&-(\mathbf{r}'\times[J_r]\{\dot{\bar{\omega}}\})'+\mathbf{F}_E+\mathbf{F}_I=m_r\ddot{\mathbf{r}}\end{aligned} \tag{4}$$

where $\mathbf{F}_I$ and $\mathbf{F}_E$ are the internal fluid force and the applied external hydrodynamic force per unit length, respectively (see Fig. 2) and m_r is the mass of the riser per unit length, and dot denotes differentiation with respect to time. $\mathbf{m}$ is the distributed couple vector induced by the asymmetric flow due to vortex shedding. It is usually negligible if we ignore the coupling of bending and torsion is weak. The mass moment of inertia $[J_r]$ is given by

$$[J_r]=\begin{bmatrix} J_{11} & 0 & 0 \\ 0 & J_{22} & 0 \\ 0 & 0 & J_{33} \end{bmatrix} \tag{5}$$

and $\dot{\bar{\omega}}$ is the angular acceleration and is obtained from the time differentiation of the angular velocity. The angular velocity $\bar{\omega}$ is computed using the appropriate transformation matrices that carry the initial system $(\hat{i}, \hat{j}, \hat{k})$ to the final triad $(\hat{n}, \hat{b}, \hat{t})$. The effective tension, T_e, is defined by

$$T_e=\hat{t}\cdot\mathbf{F} \tag{6}$$

Alternatively the effective riser tension, which is the tangential component of the internal force, may be

given approximately by (Dareing, 1976)

$$T_e \simeq T + \rho_w g\pi D_o^2 (S_w - z)/4 - \rho_m g\pi D_i^2 (S_m - z)/4 \quad (7)$$

where T=actual tension in the riser, S_w=ordinate of the free surface of water, S_m=ordinate of the free surface of mud, ρ_w and ρ_m are the densities of water and mud respectively, D_o and D_i=external and internal diameter of the riser and z is measure from the lower ball joint, i.e., $z=s+x_3$.

The actual tension T also satisfies the consitutive relation:

$$T=EA\varepsilon_t \quad (8)$$

where EA is the stretching rigidity and ε_t is the strain of the riser centerline in the tangential direction defined as

$$\varepsilon_t=\left[\frac{d\mathbf{r}}{ds}\cdot\frac{d\mathbf{r}}{ds}\right]^{1/2}-1 \quad (9)$$

where s is related to s_1 by

$$\frac{ds_1}{ds}=1+\varepsilon_t \text{ or } \frac{ds}{ds_1}=\frac{1}{1+\varepsilon_t} \quad (10)$$

For an inextensible riser, $\varepsilon_t=0$ and the deformed arclength s_1 becomes the undeformed arclength s from Eq. (10). However, Eq. (7) and Eq. (8) have to be kept to compute ε_t for the extensible riser. H represents torsional couple prescribed at end.

2.2 Force due to Internal Flow

The force acting on the internal wall of the riser is derived by using the concept of Hamilton's principle. No small-scale motions such as turbulence or secondary flow are assumed to be absent. And also, the plug-flow model with no radial variation of velocity is utilized as a fluid model for the internal flow.

Hamilton's principle in our problem states that

$$\delta\int_{t_1}^{t_2}(T_r+T_f-V_r-V_f)\,dt=0 \quad (11)$$

where, T_r and V_r are the kinetic and potential energies associated with the tube, and T_f and V_f are the corresponding quantities for the fluid. Using the velocity of the internal fluid obtained from neglecting the stretching strain, we have kinetic energy of the enclosed volume of fluid.

$$T_f=\frac{m_f}{2}\int_{s_1}^{s_2}\left[V_1+\left(\frac{\partial x_1}{\partial t}+V_1\frac{\partial x_1}{\partial s_1}\right)^2+\left(\frac{\partial x_2}{\partial t}+V_1\frac{\partial x_2}{\partial s_1}\right)^2+\left(\frac{\partial x_3}{\partial t}+V_1\frac{\partial x_3}{\partial s_1}+1\right)^2\right]ds_1 \quad (12)$$

and the potential energy of the fluid is zero because the fluid is assumed to be incompressible, i.e.,

$$V_f=0 \quad (13)$$

Performing the variation after the substitution of Eq. (12) and (13) into (11), we obtain the following integration

$$\int_{t_1}^{t_2}\int_{s_1}^{s_2}[m_f\{(\dot{x}_1+V_1x'_1)(\delta\dot{x}_1+V_1\delta x'_1)+(\dot{x}_2+V_1x'_2)(\delta\dot{x}_2+V_1\delta x'_2)+(\dot{x}_3+V_1x'_3+1)(\delta\dot{x}_3+V_1\delta x'_3)\}+\delta T_r-\delta V_r]ds_1\,dt \quad (14)$$

Since $\delta\dot{x}_i=\frac{\partial}{\partial t}(\delta x_i)$, $\delta x'_i=\frac{\partial}{\partial x_i}(\delta x_i)$ $(i=1, 2, 3)$

each terms may be integrated by parts so as to eliminate the various derivatives of δx_i. When this is done, there is obtained

$$\int_{t_1}^{t_2}\int_{s_1}^{s_2}\left[\sum_{i=1}^{3}(m_f\ddot{x}_i+2m_fV_1\dot{x}_i'+m_fV_1^2x_i'')\delta x_i+\delta T_r-\delta V_r\right]ds_1dt=0 \quad (15)$$

From the concept of the resulting Euler-Lagrange equations, we can recognize that the expression in round bracket represents the forcing components of a fluid particle inside the pipe due to internal flow. Thus, the fluid force acting on the internal wall of the pipe can be written in vector form

$$\mathbf{F}_I=-m_f(\ddot{\mathbf{r}}+2V_1\dot{\mathbf{r}}'+V_1\mathbf{r}'') \quad (16)$$

The first term on the right represents the inertia force associated with the riser acceleration. The second term is the inertia force associated with the Coriolis acceleration which arise because the fluid is flowing with velocity V_1 relative to the riser, while the riser itself has an angular velocity at any point along its length. The last term represents the inertia force associated with the change in direction of the flow velocity, owing to the curvature of the riser.

2.3 Hydrodynamic Forces

The relative motion between the pipe and the

Pipe velocity: $\mathbf{V}_P = \dot{\mathbf{r}}$

Fluid velocity (current + waves): $\mathbf{V}_F$

Relative velocity: $\mathbf{V}_R = \dot{\mathbf{r}} - \mathbf{V}_F$

Pipe tangent vector: $\hat{t}$

Tangential component of $\mathbf{V}_R$: $\mathbf{V}_{RT} = (\mathbf{V}_R \cdot \hat{t})\hat{t}$

Normal component of $\mathbf{V}_R$: $\mathbf{V}_{RN} = \mathbf{V}_R - \mathbf{V}_{RT}$

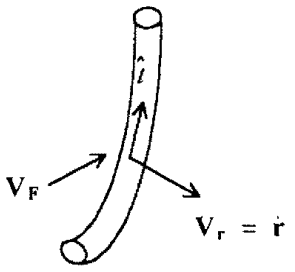

Fig. 3. Velocity vectors acting on a segment of pipe and definition of the relative velocity components.

surrounding fluid produces hydrodynamic force composed of inertia, drag, and frictional forces. The resultant total force distribution $\mathbf{F}_E$ along riser length is decomposed into a normal force component, $\mathbf{F}_N$, and a tangential component, $\mathbf{F}_T$. To perform this decomposition, the relative velocity and acceleration is resolved into components perpendicular and parallel to the deformed riser axis as shown in Figure 3. The relative velocity vector between the pipe and the surrounding fluid is given by

$$\mathbf{V}_R = \mathbf{V}_P - \mathbf{V}_C - \mathbf{V}_W = \dot{\mathbf{r}} - \mathbf{V}_C - \mathbf{V}_W \tag{17}$$

where $\mathbf{V}_P$=pipe velocity vector, $\mathbf{V}_C$=steady current velocity vector, and $\mathbf{V}_W$=time dependent wave velocity vector. It should be noted that current and wave velocity are functions of vertical position. Figure 3 depicts the velocity vectors acting on a segment of pipe and explains the definition of the relative velocity components. Noting that the current velocity is independent of time, the relative acceleration of the pipe with respect to the fluid is given by

$$\dot{\mathbf{V}}_R = \dot{\mathbf{V}}_P - \dot{\mathbf{V}}_W = \ddot{\mathbf{r}} - \dot{\mathbf{V}}_W \tag{18}$$

and its tangential and normal components are given by

$$\dot{\mathbf{V}}_{RT} = (\dot{\mathbf{V}}_R \cdot \hat{t})\hat{t} \quad \text{and} \quad \dot{\mathbf{V}}_{RN} = \dot{\mathbf{V}}_R - \dot{\mathbf{V}}_{RT} \tag{19}$$

Also, we need the tangential and normal components of the wave-induced water particle acceleration to calculate wave induced force and they are given by

$$\dot{\mathbf{V}}_{WT} = (\dot{\mathbf{V}}_W \cdot \hat{t})\hat{t} \quad \text{and} \quad \dot{\mathbf{V}}_{WN} = \dot{\mathbf{V}}_W - \dot{\mathbf{V}}_{WT} \tag{20}$$

In the present case, the tangential force component by skin friction is neglected, and only the normal force component is retained by

$$\mathbf{F}_E \approx \mathbf{F}_N = -\rho_w(\pi D_0^2/4)C_A\,\dot{\mathbf{V}}_{RN} + \rho_w(\pi D_0^2/4)\,\dot{\mathbf{V}}_{WN} - \rho_w D_0 C_D |\mathbf{V}_{RN}|\mathbf{V}_{RN}/2 \tag{21}$$

where $|\mathbf{V}_{RN}| = [V_{RN1}^2 + V_{RN2}^2 + V_{RN3}^2]^{1/2}$ and C_A=added mass coefficient, C_D=drag coefficient.

The first term of Eq. (21) is an inertia term representing the force that is required to accelerate the pipe with respect to the surrounding water. The second term is the wave induced force. This force is produced by the local pressure gradient that accompanies the normal component of water particle acceleration. The last term is the drag force that is proportional to the square of the normal velocity component and is formed by the separation of flow.

2.4 Equations of Motion and Boundary Conditions

2.4.1 Nonlinear Governing Equations

Eq. (4) is the bending equations of motion of the pipe. In this equation, H is the time dependent torque due to variation of the relative orientation of the supporting platform and imperfections of the tensioning system, and **m** is the distributed couple vector induced by the asymmetry of the flow due to vortex shedding. But **m** is usually negligible, leading to the uncoupling of the bending and torsion. Furthermore, rotatory inertia term can be neglected because the riser response is usually dominated by low frequency motion. Thus, one deduces that H is independent of the pipe length, that is, it has constant value along the riser arclength. Eq. (4) then becomes

$$-(EI\mathbf{r}'')''+[(T_e-EI\kappa^2)\mathbf{r}']'+H(\mathbf{r}'\times\mathbf{r}'')'+\mathbf{F}_t+\mathbf{F}_I = m_r\ddot{\mathbf{r}} \tag{22}$$

Substituting Eqs. (16) and (21) into the above equation,

$$\begin{aligned} m_r\ddot{\mathbf{r}}+(EI\mathbf{r}'')''-[(T_e-EI\kappa^2)\mathbf{r}']'-H(\mathbf{r}'\times\mathbf{r}'')' &= -m_f(\ddot{\mathbf{r}}+2V_f\dot{\mathbf{r}}'+V_f^2\mathbf{r}'') \\ &-\rho_w(\pi D_0^2/4)C_A\dot{\mathbf{V}}_{RN}+\rho_w(\pi D_0^2/4)\dot{\mathbf{V}}_{WN} \\ &-\rho_w D_0 C_D|\mathbf{V}_{RN}|\mathbf{V}_{RN}/2 \end{aligned} \tag{23}$$

Manipulating and letting $A_o=\pi D_o^2/4$,

$$\begin{aligned} \mathbf{q}=-\frac{1}{2}\rho_w C_D D_o|\mathbf{V}_{RN}|\mathbf{V}_{RN}+\rho_w A_o(1+C_A)\dot{\mathbf{V}}_W \\ +\rho_w A_o C_A(\hat{t}\cdot\ddot{\mathbf{r}})\hat{t}-\rho_w A_o(1+C_A)(\hat{t}\cdot\dot{\mathbf{V}}_W)\hat{t} \end{aligned} \tag{24}$$

and $m_t=m_r+m_f+\rho_w A_o C_A$ we have nonlinear governing equations (N.G.E.'s)

$$\begin{aligned} m_t\ddot{\mathbf{r}}+2m_fV_f\dot{\mathbf{r}}'+m_fV_f^2\mathbf{r}''+(EI\mathbf{r}'')'' \\ -[(T_e-EI\kappa^2)\mathbf{r}']'-H(\mathbf{r}'\times\mathbf{r}'')'=\mathbf{q} \end{aligned} \tag{25}$$

Utilization of the kinematic constraint on the unit tangent vector, $|\hat{t}|=|\mathbf{r}'|=1$, leads to the reduction of number of the unknowns. The following kinematic relations are produced from this constraint.

$$x'_3=(1-x'^2_1-x'^2_2)^{1/2}-1/(1+\varepsilon_t) \tag{26}$$

$$x_3(s_1)=x_3(0)+\int_0^{s_1}x'_3\,ds_1 \tag{27}$$

Consequently, the vertical deflections can be computed in terms of lateral one. The kinematic relations are used as predictors to remove the vertical unknowns from the governing equation. They are used again as correctors, after the solution of the reduced equations has been obtained. This will reduce the iteration or improve convergence.

2.4.2 Boundary Conditions

For the completion of the mathematical model, the boundary conditions have to be specified. The boundary conditions for the dynamic model of riser are usually time dependent because of the motions of the supporting platform. The riser support can be modeled by substituting the linear translational or rotational springs providing the restoring boundary forces and moments. Typically the displacement or the force vector and the unit tangent vector, or the bending or torsional moment has to be specified at each riser end. Figure 4 describes the free body diagram about the equilibrium of forces for the differential element at the top of the riser. From the free body diagram, equilibrium of forces at the top yields:

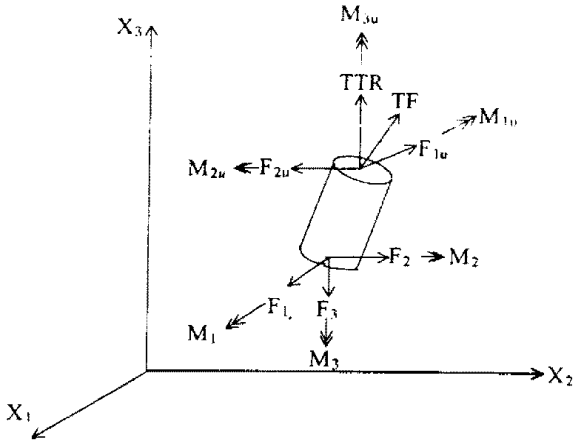

Fig. 4. Free body diagram of the equilibrium of forces and moments for the differential element at the top of the riser.

$$F_{1u}=(TF)\hat{t}\cdot\hat{i}-K_1x_{1u} \tag{28}$$

$$F_{2u}=(TF)\hat{t}\cdot\hat{j}-K_2x_{2u} \tag{29}$$

$$F_{3u}=(TF)\hat{t}\cdot\hat{k}-K_3x_{3u}+TTR \tag{30}$$

where

$$TF\approx\rho_w g\pi D_0^2(S_w-z)/4-\rho_m g\pi D_i^2(S_m-z)/4 \tag{31}$$

The subscript u indicates the upper end of the riser, TTR is the tension applied at top of the riser by the tensioning system and K_1, K_2, K_3 are spring constants supplied by the restoring boundary force. Equations (29)-(31) show that the fluidic tension at the top of the riser always acts in the tangential direction. Both TF and its direction are deformation dependent. Further more, the internal force **F** is also deformation dependent. The nonlinearity of these boundary conditions disappear in linear model because the three direction cosines in Eqs. (29)-(31) become 0, 0, and 1 respectively.

3. NUMERICAL METHOD

This paper formulates the numerical model of governing equations and boundary conditions using

finite element method. Variational statement for the boundary value problem is introduced, that is, the weak form of governing equation is derived. Sequentially, the incremental operator is applied to the weak form in order to derive the incremental equilibrium equation, and then Galerkin's decomposition method is performed to construct approximations to the solutions of the problem. Finally incorporation of the usual cubic shape functions yields the matrix dynamic equilibrium equations constructed in terms of the unknown deformations at nodal points.

3.1 Incremental Weak Form

The weak form of the mathematical model is derived in a usual manner and given as follows

$$\int_0^{l_i}\ddot{m_i}\ddot{\mathbf{r}}\cdot\bar{\mathbf{r}}ds_1+\int_0^{l_i}2m_iV_1\dot{\mathbf{r}}'\cdot\bar{\mathbf{r}}ds_1-\int_0^{l_i}m_iV_1^2\mathbf{r}'\cdot\bar{\mathbf{r}}'ds_1+\int_0^{l_i}(EI\mathbf{r}'')\cdot\bar{\mathbf{r}}''ds_1+\int_0^{l}\{(T_e-EI\kappa^2)\mathbf{r}'\}\cdot\bar{\mathbf{r}}'\ ds_1+\int_0^{l_i}\mathbf{H}(\mathbf{r}'\times\mathbf{r}'')\cdot\bar{\mathbf{r}}'\ ds_1=\{-m_iV_1^2\mathbf{r}'+\mathbf{F}\}\cdot\bar{\mathbf{r}}|_0^{l_i}-(\hat{t}\times\mathbf{M})\cdot\bar{\mathbf{r}}'|_0^{l_i}+\int_0^{l_i}\mathbf{q}\cdot\bar{\mathbf{r}}\ ds_1 \tag{32}$$

Finite approximations on the above weak form yields the matrix equilibrium equation. This is a usual procedure of the finite element approximation. However, the application of this procedure may show inaccuracy in solution or inefficiency in convergence resulted from so many iteration for the nonlinear terms in the equation. And therefore, the application of incremental operator on the weak form of governing equation (Oden, J.T., 1972) is required for the successful iteration and the incremental matrix equilibrium equation can be obtained from the incremental weak form.

Now, applying incremental operator Δ on Eq. (32) with independent variable $\mathbf{r}$ gives the incremental weak forms:

$$\int_0^{l_i}m_i\Delta\ddot{\mathbf{r}}\cdot\bar{\mathbf{r}}\ ds_1+\int_0^{l_i}2m_iV_1\Delta\dot{\mathbf{r}}'\cdot\bar{\mathbf{r}}\ ds_1-\int_0^{l_i}m_iV_1^2\Delta\mathbf{r}'\cdot\bar{\mathbf{r}}'\ ds_1+\int_0^{l_i}(EI\Delta\mathbf{r}'')\cdot\bar{\mathbf{r}}''ds_1+\int_0^{l_i}\{\Delta(T_e-EI\kappa^2)\mathbf{r}'+(T_e-EI\kappa^2)\Delta\mathbf{r}'\}\cdot\bar{\mathbf{r}}'\ ds_1+\int_0^{l_i}\mathbf{H}(\Delta\mathbf{r}'\times\mathbf{r}''+\mathbf{r}'\times\Delta\mathbf{r}'')\cdot\bar{\mathbf{r}}'ds_1=\{-m_iV_1^2\Delta\mathbf{r}'+\Delta\mathbf{F}\}\cdot\bar{\mathbf{r}}|_0^{l_i}+EI\Delta\mathbf{r}''\cdot\bar{\mathbf{r}}'|_0^{l_i}+\int_0^{l_i}\Delta\mathbf{q}\cdot\bar{\mathbf{r}}ds_1 \tag{33}$$

in which

$$\Delta(T_e-EI\kappa^2)=\Delta T_e-EI\Delta(\kappa^2) \tag{34}$$

Combine Eqs. (1), (2), and (6) into (34), we obtain

$$\Delta T_e-EI\Delta(\kappa^2)=\Delta(\mathbf{F}\cdot\mathbf{r}')-EI\Delta(\mathbf{r}'\cdot\mathbf{r}'')=\Delta\mathbf{F}\cdot\mathbf{r}'+\mathbf{F}\cdot\Delta\mathbf{r}'-2EI\Delta\mathbf{r}''\cdot\mathbf{r}'' \tag{35}$$

Substitute the result of (35) into (33), we finally get

$$\begin{aligned}&\int_0^{l_i}m_i\Delta\ddot{\mathbf{r}}\cdot\bar{\mathbf{r}}ds_1+\int_0^{l_i}2m_iV_1\Delta\dot{\mathbf{r}}'\cdot\bar{\mathbf{r}}ds_1-\int_0^{l_i}m_iV_1^2\Delta\mathbf{r}'\cdot\bar{\mathbf{r}}'ds_1\\&+\int_0^{l_i}(EI\Delta\mathbf{r}'')\cdot\bar{\mathbf{r}}''ds_1\int_0^{l_i}(T_e-EI\kappa^2)\Delta\mathbf{r}'\cdot\bar{\mathbf{r}}ds_1\\&+\int_0^{l_i}(\mathbf{F}\cdot\Delta\mathbf{r}')(\mathbf{r}'\cdot\bar{\mathbf{r}}')ds_1-\int_0^{l_i}(2EI\mathbf{r}''\cdot\Delta\mathbf{r}'')(\mathbf{r}'\cdot\bar{\mathbf{r}}')ds_1\\&+\int_0^{l_i}\mathbf{H}(\Delta\mathbf{r}'\times\mathbf{r}'')\cdot\bar{\mathbf{r}}'ds_1+\int_0^{l_i}\mathbf{H}(\mathbf{r}'\times\mathbf{r}'')\cdot\bar{\mathbf{r}}'\ ds_1\\&=\{-m_iV_1^2\Delta\mathbf{r}'+\Delta\mathbf{F}\}\cdot\bar{\mathbf{r}}|_0^{l_i}+EI\Delta\mathbf{r}''\cdot\bar{\mathbf{r}}|_0^{l_i}\\&+\int_0^{l_i}\Delta\mathbf{q}\cdot\bar{\mathbf{r}}ds_1-\int_0^{l_i}(\Delta\mathbf{F}\cdot\mathbf{r}')(\mathbf{r}'\cdot\bar{\mathbf{r}})ds_1\end{aligned} \tag{36}$$

This is the incremental weak form of the governing equation and the quantities in front of integrals are considered constants for each element so that those terms may be factored out of the integrals.

3.2 Matrix Dynamic Equilibrium Equation

The construction of a finite element approximation of the problem, such as given in (36), is based on Galerkin's decomposition method. Here, we replace (36) by a finite dimensional problem to find the approximate solution vector $\mathbf{r}_h$. The nodal values of the approximate solution are unknown functions of time and consist of not only the deflections at the nodes, but also the rotations. In other words, after constructing interpolation functions on a suitable mesh, we take the approximate solution to be of the form

$$\mathbf{r}_h=x_{1h}\hat{i}+x_{2h}\hat{j}+(x_{3h}+s)\hat{k}$$

$$\text{and } x_{jh}(s_1,\ t)=\sum_{i=1}^{4}x_{ji}(t)N_i(s_1),\qquad j=1,\ 2,\ 3 \tag{37}$$

where x_{j1}, x_{j3} and x_{j2}, x_{j4} represent the deflections and the rotations at node, and N_i is the basis or interpolation function.

Having selected the basis functions, the incremental form of an approximate solution and the test function can be written similarly

$$\Delta x_{ij}(s_1,\ t) = \sum_{i=1}^{4} \Delta x_{ij}(t) N_i(s_1)$$

$$\bar{x}_{ij}(s_1,\ t) = \sum_{i=1}^{4} \bar{x}_{ij}(t) N_i(s_1) \tag{38}$$

The substitution of (38) into (36) introduces the series form of the incremental weak form. Manipulating the series form and writing them in a matrix form, we obtain the following matrix equilibrium equation:

$$[M]\{\Delta\ddot{x}\} + [C]\{\Delta\dot{x}\} + [K]\{\Delta x\} = \{\Delta f\} + \{\Delta F\} \tag{39}$$

where,

$$[M] = \begin{bmatrix} [M_{ij}] & [0] & [0] \\ [0] & [M_{ij}] & [0] \\ [0] & [0] & [M_{ij}] \end{bmatrix} \quad [C] = \begin{bmatrix} [C_{ij}] & [0] & [0] \\ [0] & [C_{ij}] & [0] \\ [0] & [0] & [0] \end{bmatrix}$$

$$[K] = \begin{bmatrix} [K_{1ij} + K_{2ij} + K_{3ij} + K_4{}^{11}{}_{ij} + K_5{}^{11}{}_{ij}] & [K_4{}^{12}{}_{ij} + K_5{}^{12}{}_{ij} + K_6{}^{12}{}_{ij} + K_7{}^{12}{}_{ij}] & [K_4{}^{13}{}_{ij} + K_5{}^{13}{}_{ij} + K_6{}^{13}{}_{ij} + K_7{}^{13}{}_{ij}] \\ [K_4{}^{21}{}_{ij} + K_5{}^{21}{}_{ij} + K_6{}^{21}{}_{ij} + K_7{}^{21}{}_{ij}] & [K_{1ij} + K_{2ij} + K_{3ij} + K_{4ij}^{22} + K_{5ij}^{22}] & [K_{4ij}^{23} + K_{5ij}^{23} + K_{6ij}^{23} + K_{7ij}^{23}] \\ [K_4{}^{31}{}_{ij} + K_5{}^{31}{}_{ij} + K_6{}^{31}{}_{ij} + K_7{}^{31}{}_{ij}] & [K_{4ij}^{32} + K_{5ij}^{32} + K_{6ij}^{32} + K_{7ij}^{32}] & [0] \end{bmatrix}$$

$$\begin{bmatrix} [C_{cij}] & [0] & [0] \\ [0] & [C_{cij}] & [0] \\ [0] & [0] & [0] \end{bmatrix}$$

$$\{\Delta f\} = \begin{bmatrix} \{q_j{}^1 + f^1{}_{ij}\} \\ \{q^2{}_i + f^2{}_{ij}\} \\ \{q^3{}_j + f^3{}_{ij}\} \end{bmatrix} - \begin{bmatrix} \{f^1{}_{k4j} + f^1{}_{k5j} + f^1{}_{k6j} + f^1{}_{k7j}\} \\ \{f^2{}_{k4j} + f^2{}_{k5j} + f^2{}_{k6j} + f^2{}_{k7j}\} \\ \{f^3{}_{k1j} + f^3{}_{k2j} + f^3{}_{k3j} + f^3{}_{k4j} + f^3{}_{k5j}\} \end{bmatrix}$$

$$- \begin{bmatrix} \{0\} \\ \{0\} \\ \{f_{cij}\} \end{bmatrix} + \begin{bmatrix} \{0\} \\ \{0\} \\ \{f_{ccij}\} \end{bmatrix}$$

$$\{\Delta F\} = \begin{bmatrix} \{\Delta F_{1j}\} \\ \{\Delta F_{2j}\} \\ \{\Delta F_{3j}\} \end{bmatrix} \tag{40}$$

In Eq. (39), the matrix $[M]$ is a consistent mass matrix which is identical to the one derived for small deformation models and includes the added mass of the riser and the mass of the drilling fluid. $[C]$ is an anti-symmetric matrix due to the Coriolis force resulting from the internal flow. Furthermore $[K]$ is the time and deformation dependent stiffness matrix and consists of 8 components: $[K_1]$ is due to the centrifugal force from the internally flowing fluid, $[K_2]$ is the bending stiffness matrix, and $[K_3]$ is the geometric stiffness matrix which implicates the nonlinear coupling between axial tension and bending. The previous three matrices are symmetric, while $[K_4]$, $[K_5]$, $[K_6]$ and $[K_7]$ are non-symmetric, full matrixes, $[K_4]$, $[K_5]$ are due to the variable longitudinal tension and $[K_6]$, $[K_7]$ are due to the torque H. Finally, $[C_c]$ is the centrifugal force component at the both end of element. As forcing components, $\{f\}$ is the deformation dependent equivalent nodal force vector and $\{F\}$ is the internal force and moment vector.

3.3 Predictor-Corrector Scheme

The utilization of the kinematic constraint on unit tangent vector makes it feasible to represent the vertical degrees of freedom in terms of the lateral ones. This does lead to the reduction of the degrees of freedom per element from 12 to 8 and remove the possibility of the divergence in solutions due to the iteration of highly nonlinear terms in the vertical degrees of freedom. Moreover, it can be implemented as an another algorithm scheme for the iteration due to nonlinear terms. For the development of an algorithm, so called predictor-corrector scheme, the derivation of the incremental form of the extensibility condition is necessary because the equations of equilibrium for a finite element system in motion to be solved is of the incremental form.

Using the kinematic constraint on unit tangent vector of riser, i.e. $\hat{t}\cdot\hat{t} = \mathbf{r}'\cdot\mathbf{r}' = 1$, we have the following relationship:

$$x_1'^2 + x_2'^2 + (x_3' + 1/(1+\varepsilon_t))^2 = 1 \tag{41}$$

Applying the incremental operator Δ on above equation, we obtain

$$\Delta x_3' = -(x_1'\Delta x_1' + x_2'\Delta x_2')(x_3' + 1/(1+\varepsilon_t))^{-1} + \Delta\varepsilon_t(1+\varepsilon_t)^{-2} \tag{42}$$

also, we have

$$T_e = \mathbf{F}\cdot\hat{t} = \mathbf{F}\cdot\mathbf{r}' = F_1x_1' + F_2x_2' + F_3(x_3' + 1/(1+\varepsilon_t)) \tag{43}$$

Applying the incremental operator on Eq. (43), we get

$$\Delta T_e = \Delta F_1 x_1' + \Delta F_2 x_2' + \Delta F_3 (x_3' + 1/(1+\varepsilon_f)) + F_1 \Delta x_1' + F_2 \Delta x_2' + F_3 \Delta x_3' - F_3 \Delta \varepsilon_f (1+\varepsilon_f) \quad (44)$$

Also, we have

$$T_e = EA\varepsilon_f + \rho_w A_o g(S_w - S - x_3) - \rho_m A_i g(S_m - S - x_3) \quad (45)$$

Applying Δ again on Eq. (45), we obtain

$$\Delta T_e = EA\Delta\varepsilon_f - \Delta x_3 g(\rho_w A_o - \rho_m A_i) \quad (46)$$

Eliminating ΔT_e from Eqs. (44) and (46), we compute $\Delta\varepsilon_f$

$$\Delta\varepsilon_f = \{\Delta F_1 x_1' + \Delta F_2 x_2' + \Delta F_3 (x_3' + 1/(1+\varepsilon_f)) + F_1 \Delta x_1' + F_2 \Delta x_2' + F_3 \Delta x_3' + \Delta x_3 g(\rho_w A_o - \rho_m A_i)\} / \{EA + F_3 (1+\varepsilon_f)^{-2}\} \quad (47)$$

Substituting Eq. (47) into Eq. (42) and solving for $\Delta x_3'$, we obtain

$$\Delta x_3' = \left(1 + \frac{F_3}{EA(1+\varepsilon_f)^2}\right)\left[-\frac{x_1'\Delta x_1' + x_2'\Delta x_2'}{x_3' + 1/(1+\varepsilon_f)} + \frac{1}{EA(1+\varepsilon_f)^2 + F_3}\{\Delta F_1 x_1' + \Delta F_2 x_2' + \Delta F_3 (x_3' + 1/(1+\varepsilon_f)) + F_1 \Delta x_1' + F_2 \Delta x_2' + \Delta x_3 g(\rho_w A_o - \rho_m A_i)\}\right] \quad (48)$$

In addition to Eq. (48), we also have

$$\Delta x_3 = \int_0^{S1} \Delta x_3' \, ds_1$$

$$x_3' = (1 - x_1'^2 - x_2'^2)^{1/2} - 1/(1+\varepsilon_f)$$

$$x_3 = x_3(0) + \int_0^{S1} x_3' \, ds_1 \quad (49)$$

As stated earlier, the vertical degrees of freedom can be computed in terms of the lateral ones. For each load increment the kinematic relations, Eqs. (48) and (49), are used as predictors to remove the vertical degrees of freedom from global matrix equation of equilibrium. They are used again as correctors, after the solution of the reduced system of equations has been achieved. During prediction phase x_3, x_3', Δx_3, $\Delta x_3'$ are computed using Eqs. (48) and (49). In addition, during the prediction phase equation (39) are used to compute x_1, x_1', Δx_1, $\Delta x_1'$, x_2, x_2', Δx_2, $\Delta x_2'$. During the correction phase x_3, x_3', Δx_3, $\Delta x_3'$ are recomputed using Eqs. (48)-(49) and all deformation dependent matrices, the equivalent nodal forces, the boundary conditions and the lengths of elements are corrected. Further x_1, x_1', Δx_1, $\Delta x_1'$, x_2, x_2', Δx_2, $\Delta x_2'$ are recomputed using Eq. (39). This predictor-corrector scheme is repeated until convergence is achieved for each load increment. The algorithm is summarized in Figure 5.

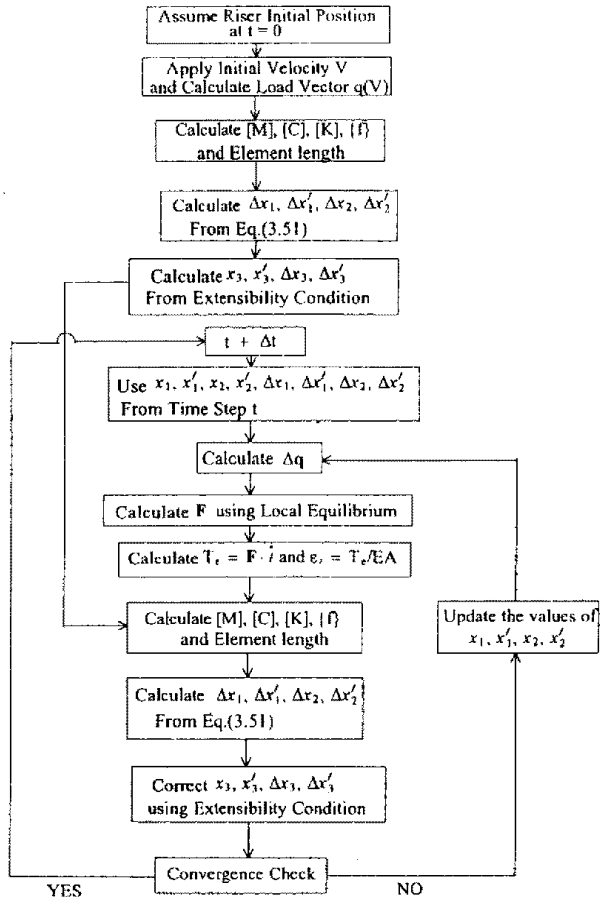

Fig. 5. Solution algorithm employing predictor-corrector Scheme.

4. THE INVESTINGATION OF THE EFFECT OF INTERNAL FLOW ON RISER DYNAMICS

4.1 Comparison between the Effects of Centrifugal and Coriolis Forces

As stated in introduction, internal flow, as it travels along the curved path in the riser, generates centrifugal and Coriolis force. These dynamic forces exerted against the riser, in turn, affect the dynamic behavior of a riser. The centrifugal force reduces the stiffness of a riser whereas the coriolis force

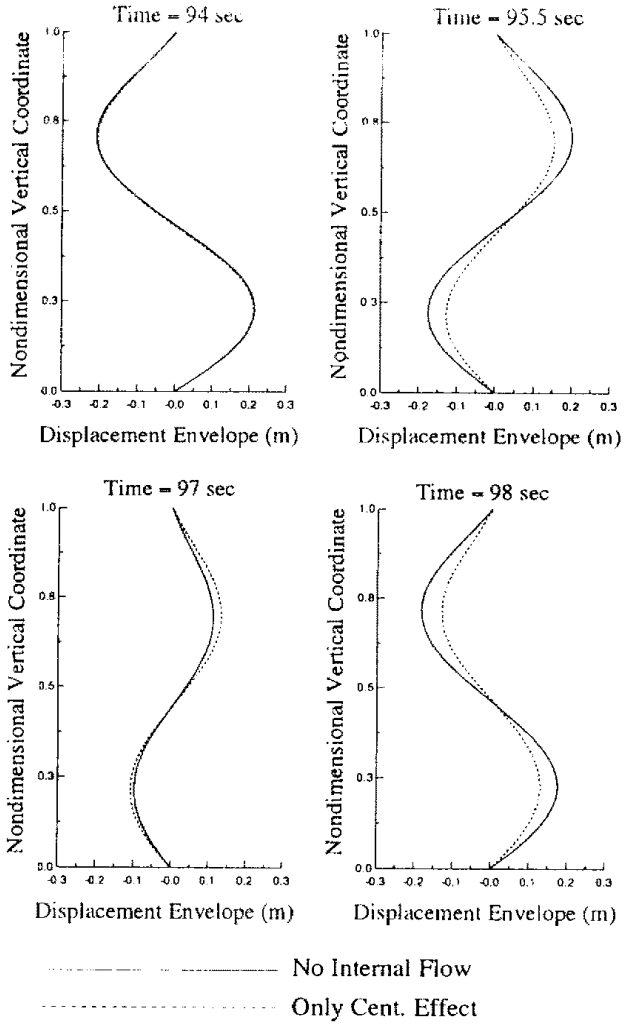

Fig. 6. The Effect of centrifugal force on displacement envelope of riser at an arbitrary time. (TR=1.2, w=3.86 kN/m, Hw=6.1 m, Tw=5 sec).

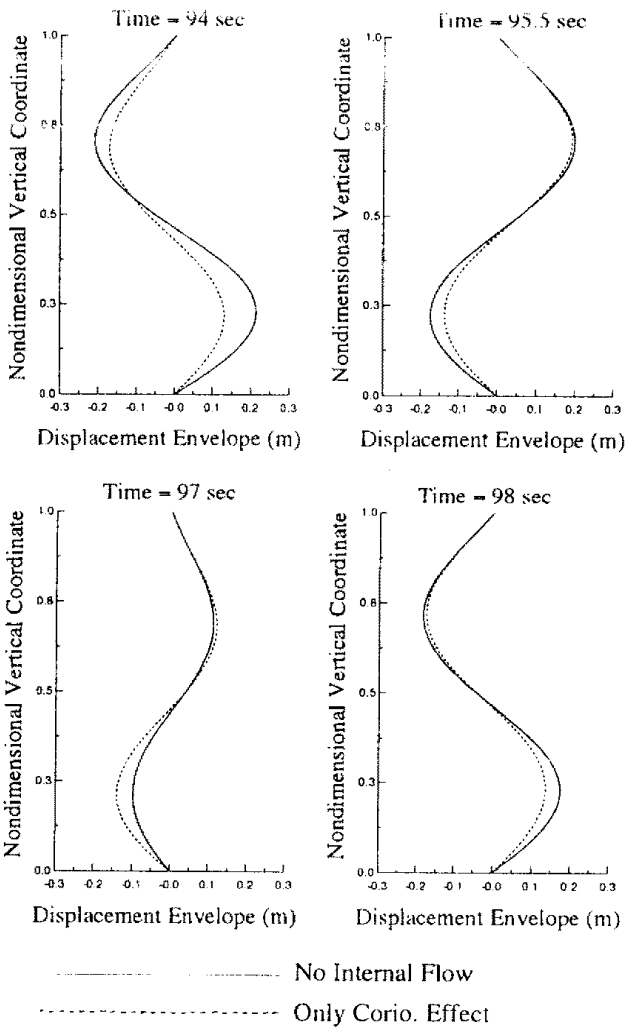

Fig. 7. The Effect of coriolis force on displacement envelope of riser at an arbitrary time. (TR=1.2, w=3.86 kN/m, Hw=6.1 m, Tw=5 sec).

causes the dynamic coupling with other forces. Their effects on riser behavior are separately examined here. Fig. 6 presents the displacement shapes of a riser at four different arbitrarily selected times to illustrate how the deflected shape changes with the inclusion of the centrifugal force only. In comparison with the no internal flow situation, the magnitude of the displacement envelopes are changed but the shapes remain undistorted. In other words, the ratio of magnification remains constant along the riser. It should be noted here, since centrifugal force reduces the stiffness of the riser, the amplitude of the riser displacement also increases with increasing centrifugal force. However, a phase diffrence is introduced into the system. Therefore, the amplitude amplification will not be manifested at every instance.

Unlike the effect of centrifugal force, the Coriolis force alters the displacement shape as shown in Fig. 7. As can be seen, the magnitudes of displacement change at upper and lower part of riser are different. This can be understood from the fact that the Coriolis force term is composed of a mixed derivative with respect to time and space or the Coriolis matrix in matrix equilibrium equation is skew symmetric. The Coriolis force alternately couples with inertia and stiffness according to the passage of time. In summary, the centrifugal force, which depends only on the curvature of riser deflection, does not alter the displacement shape, while the Coriolis force, which has a mixed derivative of time and space, distorts the displacement shape.

4.2 Consideration of Geometric Nonlinearity

The nonlicarities in riser dynamic analysis are mainly of two origins that result from the flow induced drag force and from geometric nonlinearities due to large structural deflections. In particular, the latter becomes significant for long riser. To examine the effects of geometric nonlinearity, Maximum displacements of riser with the inclusion of internal flow may be computed by the program for different riser lengths or water depths. But, there is no readily available information on selecting riser parameters for every water depth and on determining top tension value to avoid riser failure due to excessive stress. A conservative approach is taken here to let the top tension be maintained a constant value regardless of water depth and then, let the effective weight be adjusted to avoid negative tension over the riser length for different water depths. In practice, this effective weight can be adjusted by altering the buoyancy along the riser.

With this hypothetical riser, the maximum displacements of the riser are computed for water depth up to 1500 m using both linear and nonlinear models. The ratios of these maximum displacements to that of the case without internal flow are plotted in Figure 8. As shown in the figure, this maximum displacement ratio basically increases with depth to a certain peak point beyond which it decreases with depth and gradually approaches a constant as the effect of the riser stiffness also diminishes with depth. The effect due to nonlinear geometry can also be examined from this figure. As can be seen, in shallow water the effect of geometric nonlinearity is actually to reduce the displacement ratio. However, as the water becomes deeper than certain critical valuc, the displacement ratio becomes larger with the consideration of the geometrical nonliearity. The differences from the linear model and the nonlinear model clearly are not negligible and they become larger for higher internal flow velocity. For the case of increased top tension such as shown in Figure 9, the displacement ratio is also found to follow the same trend but the differences between the linear and nonliner models become smaller. In summary, the effect of geometrical nonlinearity becomes incerasingly more important for risers in

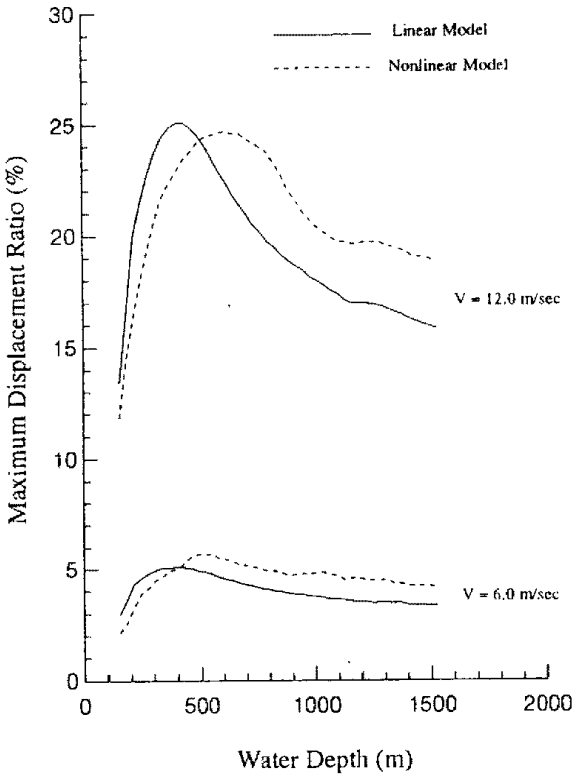

Fig. 8. Comparison between linear and nonlinear model about the effect of internal flow according to the change of water depth and internal flow velocity. top tension=650 kN, TR=1.1, effective weight= top tension/(TR×riser length).

deeper water, particularly if the top tension is low and the internal flow velocity is high. Under such conditions, linear model underestimates the displacement as compared to nonlinear model. A linear model can be used if top tension is high which generally restricts its application to shallow water.

4.3 Riser Vibrations due to Wave or Current Loading

Fist, the time simulations of tip displacements are calculated for the condition of the combined uniform current and wave system at a right angle to each other. The results are shown in Figure 10. Figure 10 shows the time dependent trajectory of riser tip displacement. As expected, the coupled response in both directions results in the narrowing pattern in the current direction but maintains a modulated oscillation in the wave direction. The presence of internal flow causes a slight decrease in current direction displacement but a more pro-

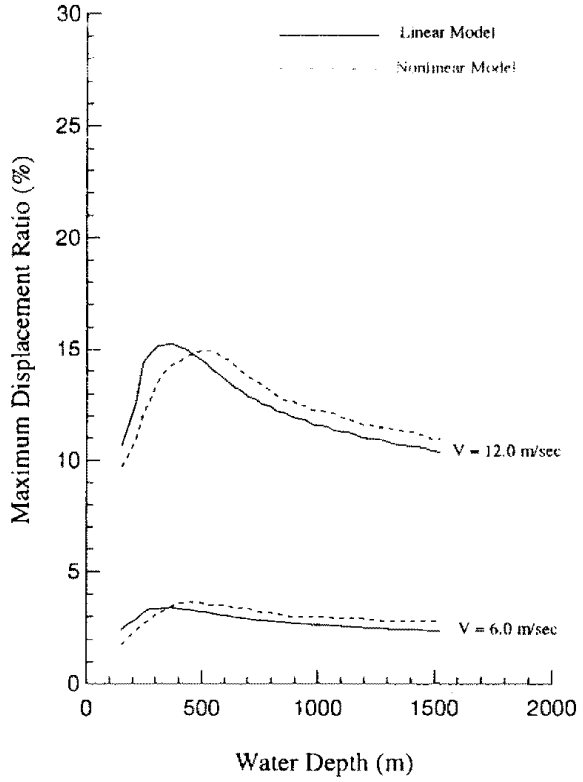

Fig. 9. Comparison between linear and nonlinear model about the effect of internal flow according to the change of water depth and internal flow velocity. top tension=765 kN, TR=1.1, effective weight= top tension/(TR×riser length).

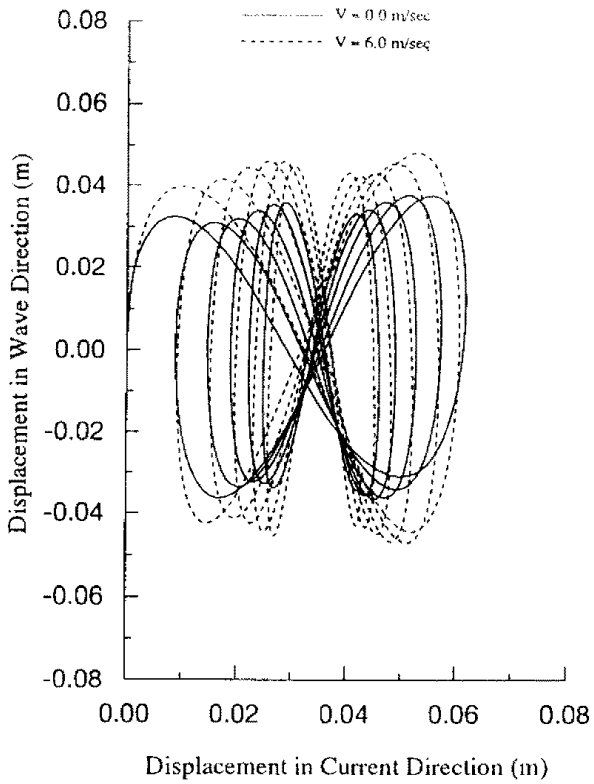

Fig. 10. The effect of internal flow on the time-dependent trajectory at the tip of 152 m riser. (current velocity U=0.4 m/sec, wave period Tw=20 sec, wave height Hw=6.1 m, top tension=350 kN, effective weight w=2.3 kN/m, semi-restrained top condition, current and wave cross with an right angle).

nounced increases in wave direction displacement. Figure 11 presents the effect of internal flow on the maximum displacement as a function of current strength for different riser tensions and internal velocities. In this case, the centrifugal force dominates the Coriolis effect and the effect of internal flow becomes larger with increasing current velocity as a result of the increased riser deformation. This effect is further magnified for risers with low tension as seen in this figure. in other words, in order to reduce the centrifugal force due to internal flow one must increase either the top tension or the buoyancy. Figure 12 plots the maximum displacement in the wave direction as a function of wave frequency for different top tensions and internal flow velocities. Displacement due to wave loading has resonance peaks of which the positions are lightly shifted due to the presence of internal flow. The effect of internal flow on tip displacement is not significant if the riser is restrained at the top by a large mass with strong damping and stiff spring.

4.4 Effects on Internal Stresses and Displacement Fields

It can be seen from Fig. 13 that the maximum effect on displacement occurs at the locations where the slopes are zero and the maximum effect on riser rotation occurs at the bottom. The effects on bending moment are the same as on displacement but the effects on shear force are not as evidenced in Figure 14. For the system under harmonic loading such as wave, the maximum effect on displacement is found at the locations where the slope is zero, while the maximum effect on rotation occurs not only at the bottom but also at the inflection points. Furthermore, the maximum effect on shear force occurs at the inflection points.

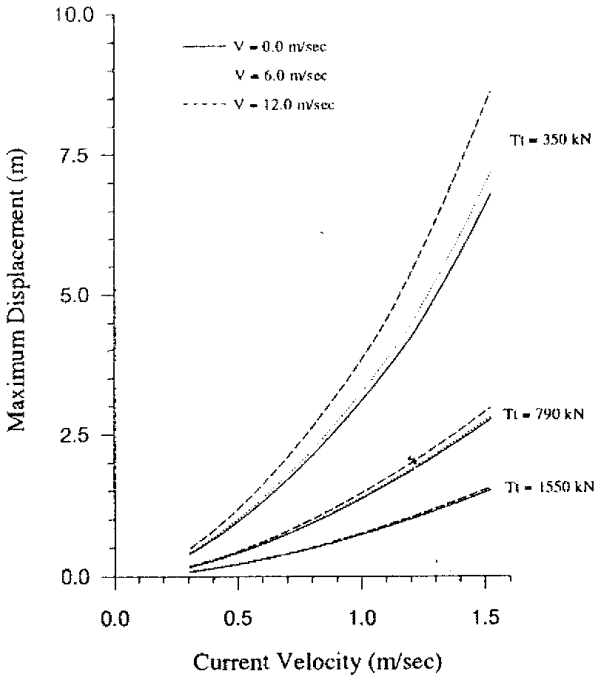

Fig. 11. The effect of internal flow on maximum displacement according to the increase of current velocity. System is same as example of Fig. 10 except parameters shown in this figure.

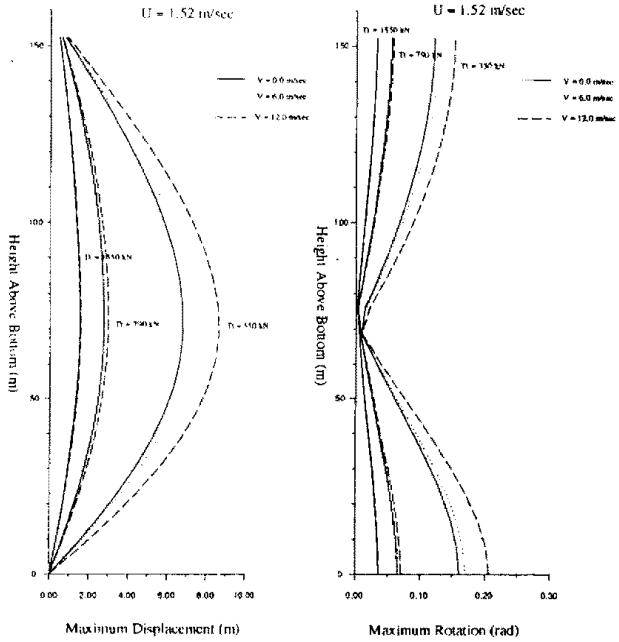

Fig. 13. The effect of internal flow on maximum displacement and rotation envelope due to current loading for three types of top tension. System is same as example of Fig. 10 except parameters shown in this figure.

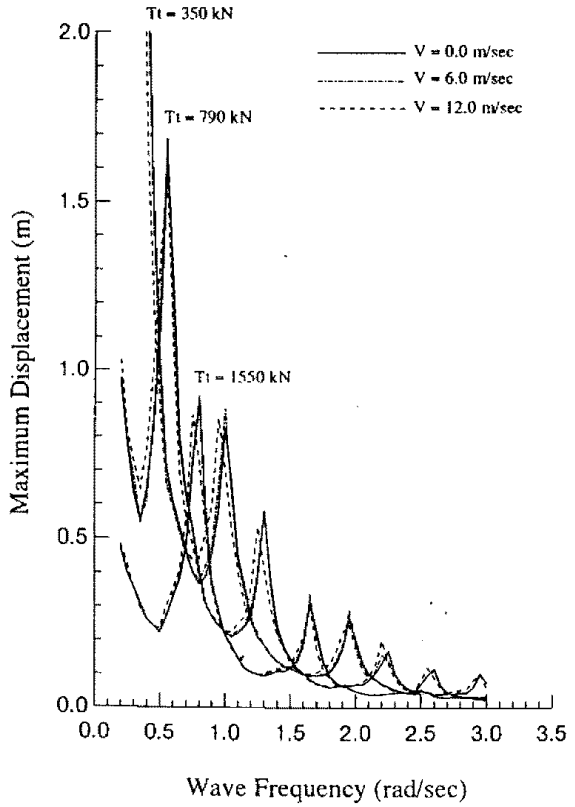

Fig. 12. The effect of internal flow on maximum displacement according to the increase of wave frequency. System is same as example of Fig. 10 except parameters shown in this figure.

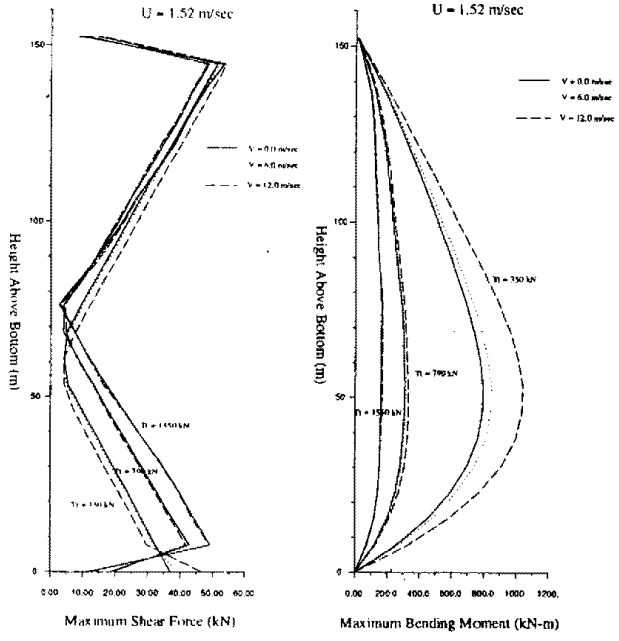

Fig. 14. The effect of internal flow on maximum shear and bending moment envelope due to current loading for three types of top tension. System is same as example of Fig. 10 except parameters shown in this figure.

5. CONCLUSIONS

A mathematical model for the analysis of riser systems with the inclusion of internal flow is developed together with numerical solutions and computer programs. From the results of sample computations, the effects of internal flow on riser dynamics are examined. The following conclusions are drawn:

1) There are two dynamic forces due to the motion of internal fluid, that is, centrifugal and Coriolis force. The centrifugal force, which depends only on the curvature of riser deflection, does not alter displacement shape where as the Coriolis force, which is a term with mixed derivative of time and space, distorts the displacement shape.

2) The effect of geometrical nonlinearity becomes increasingly more important for risers in deeper water, particularly if the top tension is low and the internal flow velocity is high. Under such conditions, the linear model understimates the displacement as compared to the nonlinear model. A linear model can be used if top tension is high which generally restricts its application to shallow water.

3) The effect of internal flow on tip displacement is not significant if the riser is restrained at the top by a large mass with strong damping and a stiff spring.

4) The effect of internal flow on the displacement of a riser in a current field is dominated by centrifugal force. On the other band, for riser under pure wave loading the internal flow effect is dominated by Coriolis force. Also, centrifugal force always increases the displacement which is undesirable, but Coriolis force could increase or reduce displacement depending on the modes of resonant peaks.

5) The effects of internal flow on maximum displacement and rotation become more important when current velocity and/or internal flow velocity increase, and when top tension decreases. In particular, the maximum effect on displacement occurs at the locations where the slopes are zero and the maximum effect on riser rotation occurs at the bottom. The effects on bending moment are the same as on displacement but the effects on shear force are not in a certain rule.

In addition to the conclusions made in this study, it should be noted that the effects of Coriolis force could be overestimated because downward internal flow is not included in the construction of a mathematical model even though the downward flow tends to reduce Coriolis force.

REFERENCES

Bernitsas, M.M. and Kokarakis, J.E., 1985, Large deformation three-dimensional static analysis of deep water marine risers, *Applied Ocean Research*, 7(4), pp. 178-187.

Bruce, E.B. and Michael, F.M., 1977. Nonlinear dynamic analysis of coupled axial and lateral motion of marine risers, *Offshore Technology Conference*, OTC 2776, Houton, Texas, pp. 403-412.

Burke, B.G., An analysis of marine risers for deep water, *Journal of petroleum Technology*, pp. 403-412.

Chakrabati, S.K. and Frampton, R.E., 1982 Review of riser analysis techniques, *Applied Ocean Research*, **4**(2), pp. 73-90.

Chen, B.C.M., 1992 A marine riser with internal flow-induced vibration, *Offshore Technology Conference*, OTC 6893, Houston, Texas, 1992, pp. 183-190.

Chung, J.S., 1981. Nonlinear transient motion of deep ocean mining pipe, *ASME Journal of Energy Resources Technology*, **103**, pp. 2-10.

Chung, J.S. and Fellipa, C.A., 1981. Noonlinear static analysis of deep ocean mining pipe-Part II: Numerical studies, *ASME Journal of Energy Resources Technology*, **103**, pp. 16-25.

Dareing, D.W. and Hung, T., 1955. Marine riser vibration response determined by modal analysis, *ASME Journal of Energy Resources Technology*, ***101***, pp. 159-166.

Fellipa, C.A. and Chung, J.S., 1981. Nonlinear static analysis of deep ocean mining pipe-Part I: Modeling and formulation, *ASME Journal of Energy Resources Technology*, **103**, pp. 11-15.

Garrett, D.L., 1982. Dynamic analysis of slender rods, *ASME Journal of Energy Resources Technoloogy*, **104**, pp. 302-306.

Hung, T. and Chucheepsakul, S., 1985. Large displacement analysis of a marine riser, *ASME Journal of Energy Resources Technology*, **107**, pp. 54-59.

Kim, Y.C. and Triantafyllou, M.kkS., 1984. The nonlinear dynamics of long, slender cylinders, *ASME Journal of Energy Resources Technology*, **106**, pp. 250-256.

Kokarakis, J.E. and Bernitasa, M.M., 1987. Nonlinear three dimensional dynamic analysis of marine risers, *ASME Journal of Energy Resources Technology*, **109**, pp. 105-111.

Konuk, I., 1982. Application of an adaptive numerical technique 3-D pipeline problems with strong nonlinearities, *ASME Journal of Energy Resources Technology*, **104**, pp. 58-62.

McNamara, J.F. and Lane, M., 1984. Practical modeling for articulated risers and loading columns, *ASME Jou-*

rnal of Energy Resources Technology. **106**, pp. 444-450.

Moe, G. and Chucheepsaku., S., 1988. The effect of internal flow on marine risers. *7th International Conference on Offshore Mechanics and Arctic Engineering*. Tokyo, Japan, pp. 375-382.

Nordgren, R.P., 1974. On computation of the motion of elastic rods. *ASME Journal of Applied Mechanics*, **96**, pp. 777-780.

Nordgren, R.P., 1982. Dynamic analysis of marine risers with vortex excitation. *Journal of Energy Resources Technology*, **104**, pp. 14-19.

O'Brien, P.J. and McNamara, J.F., 1988. Three dimensional nonlinear motions of risers and offshore loading towers. *ASME Journal of offshore Mechanics and Arctic Engineering*, **110**, 00. 232-237.

Oden, J.T., 1972. *Finite Elements of Nonlinear Continua*. McGraw Hill Co., New York.

Safai, V.M., 1983. Nonlinear dynamic analysis of deep water risers. *Applied Ocean Research*, **5**(4), pp. 215-225.

Wu, M.C. and Lou, J.Y.K., 1991. Effects of rigidity and internal flow on marine riser dynamics. *Applied Ocean Research*, **13**(5), pp. 235-244.